This article has been accepted for publication in IEEE Transactions on Power Electronics. This is the author's version which has not been fully edited and content may change prior to final publication. Citation information: DOI 10.1109/TPEL.2025.3531695

Digital Twins in Power Electronics: A Comprehensive Approach to Enhance Virtual Thermal Sensing

R. Torchio, F. Conte, M. Scarpa, M. Filippini, F. Pase, F. Toso, P. Shahriari Nasab, E. Marson, A. Viroli, P. Posa, M. Zangoli

***Abstract*—The traditional approaches in material research and hardware design are insufficient to address the evolving Operation and Maintenance (O&M) demands in contemporary power electronics. Overengineering and data acquisition practices lead to unsustainable costs and reduced profit margins. Digital Twins (DTs), defined as real-time simulation models of physical systems, emerge as promising solutions to meet stringent O&M requirements. In power electronics, DTs offer significant potential in thermal management, crucial for control performance, safety, and system lifespan. This paper aims to analyze the development of computationally efficient and high-fidelity DTs tailored for power electronics applications, emphasizing their predictive reliability of critical temperatures. The proposed physics-based approach is enhanced by integrating data-driven Artificial Intelligence (AI)-based techniques to achieve this goal. The predictive reliability of the DTs produced through this workflow is then experimentally validated for a power electronic converter designed for induction heating applications. Experimental results show that the integration of data-driven AI-based techniques allows for maintaining very high predictive accuracy even when multiple semiconductor component suppliers are considered for the same product, which is often the case for industrial products. Additionally, by implementing and executing the DT in a low-power microprocessor, the real-time execution is demonstrated, affirming its practical applicability.**

***Index Terms*—Digital Twins (DTs), Power Converters, Real-Time, Physics-Based, Data-Driven, Artificial Intelligence (AI), Virtual Thermal Sensing (VTS), edge computing.**

I. Introduction

TRADITIONAL approaches in material research and hardware design are no longer sufficient to meet the evolving Operation and Maintenance (O&M) requirements of contemporary power electronics products and systems. The prevailing industrial practice involves overengineering components and acquiring extensive data, leading to unsustainable costs and diminished profit margins.

R. Torchio and F. Conte are with the Department of Industrial Engineering of the University of Padova, Padova, 35131, Italy (email: riccardo.torchio@unipd.it, filippo.conte@studenti.unipd.it).

R. Torchio and M. Scarpa are with the Department of Information Engineering of the University of Padova, Padova, 35131, Italy (email: mattia.scarpa@studenti.unipd.it).

M. Filippini, F. Pase, and F. Toso are with Newtwen, Padova, 35127, Italy (email: mattia.filippini@newtwen.com, francesco.pase@newtwen.com, francesco.toso@newtwen.com).

P. Shahriari Nasab, E. Marson, and P. Posa, are with Electrolux Italia, Porcia, 33080, Italy (email: pedram.shahriari-nasab@electrolux.com, enrico.marson@electrolux.com, paolo.posa@electrolux.com).

A. Viroli and M. Zangoli are with Electrolux Italia, Forlì, 47122, Italy (email: alex.viroli@electrolux.com, massimo.zangoli@electrolux.com).

The emergence of Digital Twins (DTs), characterized as mathematical models capable of real-time simulation of a system's physical behavior, stands out as the most promising solution to address the increasingly stringent O&M demands in the power electronics market [1]. The maturation of enabling technologies that unify hardware and software has ushered in a new era, focusing on two key performance indicators (KPIs): enhancing maximum functionality through control performance [2] and enabling more precise and effective predictive maintenance through increased information [3].

Specifically within the domain of power electronics, the most promising area for DT technology lies in thermal management [4]–[6]. Temperature, particularly junction temperature (T_j), significantly influences control performance, safety, costs, efficiency, and system lifespan [7]–[12]. While manufacturers invest in advanced materials (e.g., SiC, GaN) to maximize power density and minimize losses, a critical challenge remains in the thermal management of these modules [13]–[15].

Current thermal management relies on sensors like Negative-Temperature-Coefficient (NTC) ones placed away from the die junctions for engineering reasons, resulting in latency and imprecise observations of junction temperature dynamics [16], [17]. This complicates the implementation of high-performance thermal management control by system manufacturers, who are forced to adopt oversized safety margins, thereby flattening the added value and competitive advantage of utilizing, for example, SiC Mosfet-based modules over IGBTs ones.

Another critical reason for the importance of junction temperature is aging models based on, e.g., physics-based models or in situ thermal impedance spectroscopy, coveted by power electronics system manufacturers for providing predictive maintenance services, enhancing product safety, and optimizing warranty periods [18]. Currently, the most accurate and reliable aging models are in the hands of semiconductor module manufacturers, performing power cycles (PC) and temperature cycles (TC) to extract empirical and physics of failure aging models [19]. These models estimate the remaining useful life (RUL) of modules, classify major fault types (e.g., solder junction wear, wire-bond lift-off, etc.), and depend on the junction temperature variation in a cycle (ΔT_j) [19].

Various methods exist for measuring junction temperature, but they are rarely implemented in production [6]. Despite module suppliers providing valuable aging models, system builders struggle to utilize them due to the difficulties to estimate junction temperature in industrial setting. Hence,

This article has been accepted for publication in IEEE Transactions on Power Electronics. This is the author's version which has not been fully edited and content may change prior to final publication. Citation information: DOI 10.1109/TPEL.2025.3531695

real-time estimation of Tj becomes crucial. While literature explores various real-time junction temperature estimation methods for power modules [20]–[25] based, e.g., on temperature-sensitive electrical parameters (TSEPs) or temperature-sensitive optical parameters (TSOPs), there lacks a structured and unified methodology poised to become an industry standard, a fundamental piece in constructing a DT for thermal management and predictive maintenance of power electronics systems.

When thermal sensing techniques must be avoided, the current state-of-the-art for junction temperature estimation remains thermal network models [18], with limitations, especially for complex systems. Designing a thermal network model without knowledge of the component geometry and without relying on experimental data, i.e., without reverse engineering the power module, is challenging. Some power module manufacturers provide thermal models for T_j estimation, but coupling them to the entire system and the heat exchange model proves difficult. Thermal networks lose physicality since the heat equation is not well represented by an equivalent lumped circuit. High-resolution thermal networks compromise real-time implementation, rendering them computationally burdensome. Designing them is mostly a manual process, requiring expertise that few engineers possess in companies. Certain simulation software companies (e.g., Ansys, Siemens, Newtwen) are investing in tools capable of reducing complex models like finite element models (FEM) into Reduced Order Models (ROM) [26]. These ROMs can be implemented on third-party hardware platforms for real-time execution, striking a balance between accuracy and computational complexity [27].

A DT transcends a real-time model estimating junction temperature. It must adapt to changes such as different operating conditions, the stochastic nature of real devices, and manufacturing errors, exchanging data bidirectionally with the real system through sensors. The DT can be used to take control actions, predict scenarios, optimize control actions, identify anomalies and hazardous conditions, and generate a wealth of information to enhance future design and predictive maintenance models [28]. In this paper, we intend to analyze the entire workflow for constructing a DT capable of providing the functionalities necessary to improve real-time control performance and thermal management. It is important to note that, in this paper, aging and degradation phenomena are not addressed, as the primary focus is on real-time monitoring of critical temperatures to support advanced thermal control strategies, also dealing with the stochastic nature of electronic components.

The remainder of the paper is organized as follows. In Section II, the workflow for generating hybrid physics- and data-driven Artificial Intelligence (AI)-based DT is described. In particular, the electric, thermal, and fluid-dynamics modeling is discussed in Section II-A. Model Order Reduction (MOR) techniques to reduce the computational cost of the physics-based models and allow their real-time execution are discussed in Section II-B. AI-based techniques to improve the accuracy of the models in working conditions are described in Section II-C, while the on-chip implementation of the final DT is described in Section II-D. The proposed approach is validated against a power electronic converter designed for induction heating applications in Section III and conclusions are given in Section IV.

II. Digital Twin Generation Procedure for Power Electronics Components

In this section, a thorough discussion is conducted on the principal constituents of a DT, encompassing its structure, implementation methodologies, and operational paradigms. Initially, the DT is founded solely upon the physics information about the constituent entity, comprising geometric specifications, material characteristics, and mathematical models delineating its physical dynamics. Subsequent phases necessitate the compression of this informational reservoir to allow real-time execution of the model on a designated microcontroller. To this end, the application of MOR techniques is imperative, ensuring an optimal equilibrium between model fidelity and computational exigency, particularly concerning memory allocation and computational complexity inherent to the microcontroller environment [29].

The key feature that sets a Digital Twin (DT) apart from a high-fidelity model is its ability to be deployed on cloud or edge hardware for real-time execution—or faster-than-real-time execution when predictions are required. This capability facilitates a dynamic exchange of information between the physical asset (e.g., the power converter) and its corresponding DT. Since, in this paper, DTs are aimed at the real-time monitoring of critical quantities, in-cloud implementations alone may not be a reliable solution, due to unavoidable communication delays. Fortunately, the recent advancements in microprocessor technology pave the way for on-chip DTs, where the digital replicas are directly embedded in the onboard available hardware.

Following the reduction process, incorporating a stochastic element rooted in empirical data is essential to reduce discrepancies between the physics model and real-world phenomena. These discrepancies typically stem from uncertainties in parameters, dynamic and time-evolving boundary conditions, and approximations introduced by the reduction strategies. The stochastic nature of electronic components is further exacerbated by the shortage issues faced by industries, making it essential to secure multiple semiconductor component suppliers. However, this increases the variability of device performance, making monitoring and control increasingly challenging. In this study, three different suppliers of discrete components were adopted. However, validating and certifying firmware with three different DT systems, each tailored to a different semiconductor module supplier, proves to be cumbersome. Therefore, developing a single integrated model that accurately and reliably represents a power electronic system potentially employing components from various suppliers in serial production poses a technological challenge.

Given the stochastic nature of electronic components production described above, combining data-driven models with physics-based ones creates a strong hybrid approach that improves the accuracy and generalization of power electronic device models [30], [31]. Upon deployment within a microcontroller framework, the resultant hybrid model furnishes

This article has been accepted for publication in IEEE Transactions on Power Electronics. This is the author's version which has not been fully edited and content may change prior to final publication. Citation information: DOI 10.1109/TPEL.2025.3531695

real-time insights of both quantitative and qualitative nature, informing control strategies with critical information such as the identification of temperature hot spots, often situated within inaccessible points like die junctions, thermal exchange dynamics with cooling system, and temporal temperature prognostications. Moreover, the expansive repository of real-time insights can be used to enhance analytical capabilities, particularly concerning degradation and aging metrics, thereby expediting the acquisition of a predictive maintenance model.

A. High Fidelity Models

The model of a Power Converter module has an intrinsically multi-physics nature since, in general, electric, thermal, and fluid dynamic effects must be considered to define the overall behavior of the device. With the final objective of generating an embeddable and thus computationally cheap DT of the device for the real-time monitoring of critical quantities (e.g., temperature), dedicated modeling strategies must be used to consider these three physics and the coupling between them.

1) Electric (Loss) Model: The Electric Loss model of the power converter relies on either datasheet specifications or experimental measurements. The methodology, as explicated in [32], delineates a systematic approach to assess both switching and conduction losses.

Conduction power losses are computed by directly multiplying the collector current (I_C) by the corresponding voltage (U_{CE}) from the datasheet, thereby determining $P_{V,COND}$ depending on the current. Furthermore, the method's advantage lies in accurately approximating the loss function with second order polynomial fitting.

Junction temperature dependency becomes paramount in estimating losses dynamically varying with the component's temperature and, so, temperature-dependent coefficients can be incorporated into the polynomials:

$$P_{V,COND}(I_C, T_j) = c \cdot I_C + d \cdot I_C^2, \tag{1}$$

where c and d are, in case of a 2nd order polynomial fitting:

- $c(T_j) = c_0 + c_1 \cdot T_j + c_2 \cdot T_j^2$
- $d(T_j) = d_0 + d_1 \cdot T_j + d_2 \cdot T_j^2$

with c_i and d_i to be defined, see [32]. The accuracy increases with a greater number of recorded operating temperatures, allowing for a higher-order approximation.

Switching losses in power electronics are dependent on variables such as current, junction temperature, operating voltage, and switching frequency. An effective evaluation procedure begins by extracting the total switching energy ($E_{tot} = E_{on} + E_{off}$) from referenced datasheets, and subsequently, the power loss expression is derived from this data. Then, these losses are systematically correlated with the respective variables, employing a method similar to that utilized for conduction losses. [32]

2) Thermal Model: The thermal model of a Power Converter must be capable of providing the dynamic evolution of the temperature in critical points of interest, e.g., the junction temperature. The thermal model is described by the following well-known advection–diffusion equation, i.e.,

$$\rho c_p \frac{\partial T}{\partial t} + \rho c_p \mathbf{v} \cdot \nabla T - \nabla \cdot k \nabla T = q, \tag{2}$$

where ρ is the density, c_p is the heat capacity at constant pressure, T is the temperature, k is the thermal conductivity, q is the power density, and $\mathbf{v}$ is the velocity field (which is not zero only in the fluid region). Power losses, i.e., q, are obtained from the Electric (Loss) Model described in Section II-A1 and the velocity field $\mathbf{v}$ of the coolant (if any) is provided by the Fluid Dynamic Model described in Section II-A3.

In (2), the dependence w.r.t. the position has been omitted for simplicity. Equation (2) is then complemented by boundary conditions valid on the border of the model ($\partial\Omega$), e.g., Dirichlet, Neumann, or, more frequently used, convective condition, i.e.,

$$\mathbf{n} \cdot k \nabla T = h(T_{ext} - T), \tag{3}$$

where $\mathbf{n}$ is the unit normal vector of the boundary of the motor, h is the convective coefficient, and T_{ext} is the external/ambient temperature. Depending on the case, radiation boundary conditions can be included too. However, considering them makes the problem non-linear, and this is in general avoided. The interested reader can refer to [33] for more details.

To generate a numeric dynamic model of (2) (including boundary conditions), Finite Element Method (FEM) is the most widely used approach. Thus, a computational model of the Power Converter is generated and a mesh is constructed. The discretized model can be finally written as [34]

$$\mathbf{M}\frac{d\mathbf{x}}{dt} + (\mathbf{K} + \mathbf{K}_{adv} + \mathbf{H})\mathbf{x} = \mathbf{Q_p}\mathbf{p} + \mathbf{Q_c}T_{ext}, \tag{4}$$

where $\mathbf{M}$ is the mass matrix, while $\mathbf{K}$, $\mathbf{K}_{adv}$, and $\mathbf{H}$ are the stiffness matrices related to conductive, advective, and convection terms, respectively. $\mathbf{p}$ is the power loss array of dimension N_p storing the losses (in [W]) for each domain (see Section II-A1), $\mathbf{Q_p}$ is the $N \times N_p$ matrix which maps $\mathbf{p}$ into the rhs of the thermal model, and $\mathbf{Q_c}$ is the array mapping the external temperature T_{ext} into the rhs of the thermal model related to the convective boundary condition.

When the device is liquid-cooled and therefore the advection term is included, it is well known that advection-dominated computational models such as the one in (4) are particularly challenging from the numerical point of view: even fine meshes lead to Peclet number $Pe > 1$, which results in large node to node oscillations. To remove such oscillations, standard stabilization techniques can be adopted (e.g., based on Streamline Upwind Petrov Galerkin (SUPG) [35]). Alternatively, one can eliminate the advective term from the thermal model and replace it with equivalent boundary conditions, specifically convective boundary conditions featuring a substantially high convective coefficient [36]. While this approach streamlines the computational complexity of the model, it concurrently compromises the model's physics accuracy. Finally, (4) can be recast into state-space (descriptor) form, i.e.,

$$\begin{aligned} \mathbf{E}\frac{d\mathbf{x}}{dt} &= \mathbf{A}\mathbf{x} + \mathbf{B}\mathbf{u} \\ \mathbf{y} &= \mathbf{C}\mathbf{x} \end{aligned}, \tag{5}$$

where $\mathbf{E} = \mathbf{M}$, $\mathbf{A} = -(\mathbf{K} + \mathbf{K}_{adv} + \mathbf{H})$, $\mathbf{B} = [\mathbf{Q_p}, \mathbf{Q_c}]$, and $\mathbf{u} = [\mathbf{p}; T_{ext}]$ is the input vector. $\mathbf{y}$ is a vector storing the temperature of interest and $\mathbf{C}$ is the corresponding matrix that computes $\mathbf{y}$ from $\mathbf{x}$. Equation (4) is recasted into (5) to allow

This article has been accepted for publication in IEEE Transactions on Power Electronics. This is the author's version which has not been fully edited and content may change prior to final publication. Citation information: DOI 10.1109/TPEL.2025.3531695

using MOR approaches (described in the next paragraph) that usually start from a state-space representation of the problem.

It is worth noting that a reduced-order thermal model can also be derived from experimental data using data-driven approaches such as Vector Fitting [37], where a state-space model is constructed directly from the data. Alternatively, a circuit-equivalent behavioral model can be employed, utilizing thermal network representations like Foster or Cauer models [38].

Regarding offline computational costs, this approach can be advantageous since no FEM model needs to be constructed, making it suitable for temperature monitoring without considering correlations or requiring model parameterization. However, adding these features would necessitate enforcing physical constraints, which expert engineers can do with a deep understanding of the device's thermal behavior. Therefore, depending on the specific application, both a FEM-based approach with order reduction and a data-driven generation of a reduced-order model are viable methods for creating a reduced order thermal model.

3) Fluid Dynamic Model: Often, Power Converters for high-power applications such as automotive ones have active cooling systems to dissipate the heat generated, e.g., based on forced fluid or air flows. Fluids allow to reach higher power densities but generally require a more expensive and complex system (pumps, filters, radiators), thus, when possible, the forced-air solution is preferred. A computational fluid dynamics (CFD) simulation is required to study the velocity and pressure distribution in the fluid domain. Time domain simulations at different flow rates generally can be carried out under the following assumptions:

- in-compressible fluid flow: this simplification is true for fluids and could be adopted also for gases when there are mild pressure changes and temperature variations;
- turbulent flow: $k-\omega$ Reynolds-averaged (RANS) turbulence model;
- wall functions with quadrangular fluid boundary mesh;
- P1 + P1 discretization of velocity and pressure;
- Streamline + crosswind diffusion numerical stabilization;

For instance, the $k-\omega$ formulation based on turbulent kinetic energy k and specific dissipation rate ω can be used:

$$\begin{cases}\rho\frac{\partial k}{\partial t}+\rho(\mathbf{u}\cdot\nabla k)=P_k-\rho\beta^*k\omega+\nabla\cdot(\mu\sigma^*\mu_T\nabla k)\\ \rho\frac{\partial\omega}{\partial t}+\rho(\mathbf{u}\cdot\nabla\omega)=\alpha\frac{\omega}{k}P_k-\rho\beta\omega^2+\nabla\cdot(\mu\sigma\mu_T\nabla\omega)\end{cases} \tag{6}$$

For the full definition of symbols, the reader is referred to [39]. It is worth mentioning that such simulations can result in high computational effort since the formulation is nonlinear and fine meshes are needed to achieve convergence. Because of these complexities, a common simplified approach is to entirely avoid the CFD simulation by substituting the coolant/wall heat exchange with an equivalent condition as previously mentioned [36].

B. Model Order Reduction

Obviously, due to their large dimension, the high-fidelity models described in the previous section are not directly compatible with the on-chip implementation. MOR techniques can be used to solve this problem.

While the Electric (Loss) model is already compatible with the on-chip implementation, for the real-time monitoring of critical quantities such as the junction temperature, the discretized state-space thermal model, i.e., (5), must be solved in real-time. A thermal model of a realistic Power Converter module resulting from FEM discretization may have thousands or even millions of unknowns. Thus, its dimensionality must be reduced to allow on-chip implementation. To do that, MOR strategies based, e.g., on Balanced Truncation [40]–[42], Moment Matching [43], or Proper Orthogonal Decomposition can be used. The interested reader is referred to, e.g., [44] for more details about different MOR strategies, which can be applied to both continuous or discrete models. Regardless of the adopted technique, MOR allows for projecting the original Full Order Model (FOM) (5) into a reduced order space, i.e.,

$$\begin{gathered}\hat{\mathbf{E}}\frac{d\hat{\mathbf{x}}}{dt}=\hat{\mathbf{A}}\hat{\mathbf{x}}+\hat{\mathbf{B}}\mathbf{u}\\ \mathbf{y}=\hat{\mathbf{C}}\hat{\mathbf{x}}\end{gathered}, \tag{7}$$

where $\hat{\mathbf{E}}=\mathbf{V}^*\mathbf{E}\mathbf{V}$, $\hat{\mathbf{A}}=\mathbf{V}^*\mathbf{A}\mathbf{V}$, $\hat{\mathbf{B}}=\mathbf{V}^*\mathbf{B}$, and $\hat{\mathbf{C}}=\mathbf{C}\mathbf{V}$ are obtained by projecting the corresponding FOM matrices into the reduced order space, while $\hat{\mathbf{x}}$ is the reduced order state, i.e., $\mathbf{x}\approx\mathbf{V}\hat{\mathbf{x}}$. $\mathbf{V}$ is the projection matrix constructed by the adopted MOR strategy. The Reduced Order Model (7) can be finally discretized in time by applying, e.g., a backward Euler scheme. It is worth noting that more advanced time-stepping techniques may be applied to discretize (7). However, advanced time-stepping techniques may not be compatible with the final on-chip implementation of the DT. The backward Euler scheme is instead simple enough to be implemented in a standard microprocessor and, by choosing a small enough value of the time step, a good level of accuracy can be guaranteed.

Concerning the fluid dynamic model, it is worth noting that the computational effort for this kind of simulation is high, which poses challenges to obtaining a reduced CFD model that can be computed in real-time. Fortunately, in industrial applications, the flow rate is kept constant, or it varies in a prescribed limited range. Thus, the velocity field $\mathbf{v}$ (which is used for the advection term of the thermal model) can be evaluated offline for a set of prescribed conditions and the thermal model can be parameterized to consider different cooling conditions. Of course, this may introduce an unavoidable approximation but allows for avoiding solving in real-time the CFD problem, which may be unfeasible for on-chip implementation. It is worth noting that the literature about MOR for CFD problems is vast and constantly growing [45], [46]. However, due to the complex nature of the CFD problems, incorporating fluid-dynamics ROMs in standard microprocessors for real-time solutions is still a challenge.

C. From Model as Designed to Model as Manufactored

This section elucidates a pivotal aspect of the research, pivotal in clarifying the essence of the DT concept within power electronics. Initially, a model, no matter how complex it is, remains an approximation of reality, encountering several challenges in representing the complete dynamics of power electronic systems [47]. These challenges include geometric

This article has been accepted for publication in IEEE Transactions on Power Electronics. This is the author's version which has not been fully edited and content may change prior to final publication. Citation information: DOI 10.1109/TPEL.2025.3531695

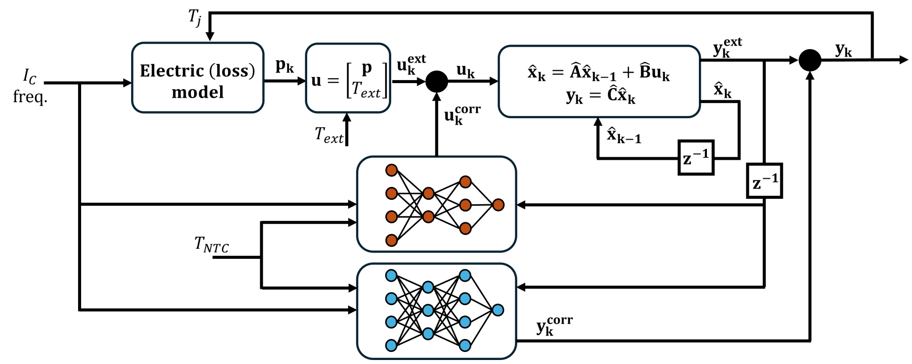

Fig. 1: Hybrid Model Architecture.

approximations, limitations of numerical methods in solving partial differential equations governing thermal and electric phenomena, uncertainties in material properties, and the approximations introduced by MOR techniques. Moreover, manufacturing processes introduce unique characteristics into each electronic component, further complicating model fidelity. Additionally, aging, wear, and operational conditions make material parameters time-varying, posing additional modeling challenges. Finally, real power-electronics products often integrate semiconductor components from multiple suppliers to address supply shortages. Consequently, products that incorporate semiconductor components from different suppliers will exhibit varying thermal behaviors. However, the DT must be unique (as tailoring a DT to specific semiconductor suppliers would be problematic in production) and must provide highly predictive accuracy for any product that includes semiconductor components from different suppliers, i.e., the temperature predicted by DT must closely align with the actual temperature of the real component.

To address these complexities, a comprehensive methodology is proposed, adopting physics-based and data-driven approaches. This hybrid model architecture aims to enhance accuracy and robustness in monitoring and controlling power electronic systems, particularly when integrated within the control and management units.

The proposed hybrid model architecture integrates a reduced physics-based model with two Feed Forward Neural Networks (FFNNs). The first FFNN serves to correct uncertainties in the thermal model's inputs, while the second FFNN corrects the thermal model's output, effectively mitigating errors in the physics-based model.

Fig. 1 shows the scheme of the hybrid DT, which integrates the physic-based and the AI-based models. As can be seen, inputs of the two FFNNs are: the inputs of the electric loss model, the (retarded) estimated output of the thermal model, and the real-time measurements from NTC sensors implemented in the system (T_{NTC}). By incorporating T_{NTC} as an input to the hybrid DT, the model gains insight into the stochastic behavior of the real-world component, such as variations in semiconductor elements and boundary conditions.

Training FFNNs involves optimizing model parameters and employing techniques such as gradient-based optimization, regularization methods, and dropout to prevent overfitting. Widely-used frameworks such as PyTorch and TensorFlow provide a robust ecosystem for FFNN development, offering flexibility, extensive support, and efficient computation. Careful selection and application of optimization algorithms, regularization techniques, and appropriate libraries are essential for effective training and calibration of FFNNs tailored to power electronic applications.

Ensuring the generalization capability of the final model architecture is paramount for robust performance in real-world power electronic applications. Integrating physics-based models with FFNN architectures enhances interpretability and promotes better generalization to unseen data by incorporating domain knowledge and fundamental principles. Maintaining physical constraints within the model architecture prevents overfitting and increases reliability, enhancing confidence in the model's performance across diverse operating scenarios and environmental conditions.

D. On Chip Implementation

The last step, which is crucial to defining the DT as such, involves real-time implementation on a microcontroller, specifically on the hardware platform controlling the actual converter. Once this step is achieved, the DT and its corresponding real counterpart have the ability to exchange data and information in a bidirectional flow through sensor readings and control actions. Therefore, it is important to ensure the following functionalities: synchronization of feedback and control actions with the integration time step of the DT, which partly consists of a state-space system to be integrated over time; stability properties of the final DT architecture, e.g., checking the eigenvalues of the state matrix; and finally, numerical conditioning of the model matrices to avoid truncation and rounding errors when implementing the model in a fixed-point 32-bit architecture, for example.

III. Case Study: Power Converter for Induction Heating Applications

A. Test Case Description

In this section, we describe the experiments conducted to test and validate the effectiveness of the DT in representing the physical behavior of a power electronic converter for induction

This article has been accepted for publication in IEEE Transactions on Power Electronics. This is the author's version which has not been fully edited and content may change prior to final publication. Citation information: DOI 10.1109/TPEL.2025.3531695

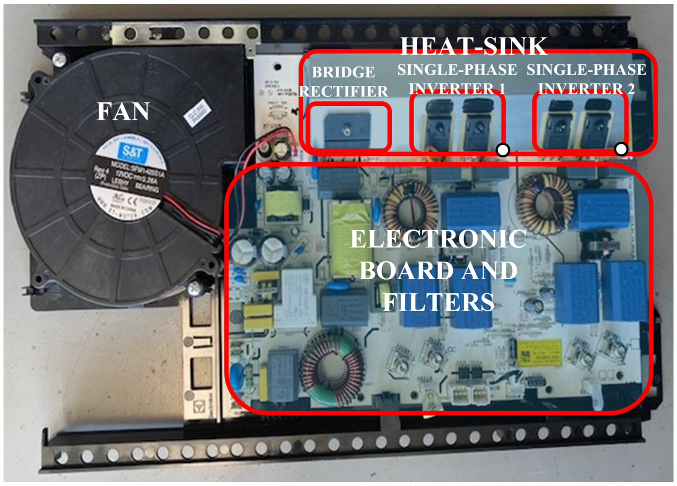

Fig. 2: Power converter without cover. The withe dots indicate the positions of the two NTC sensors.

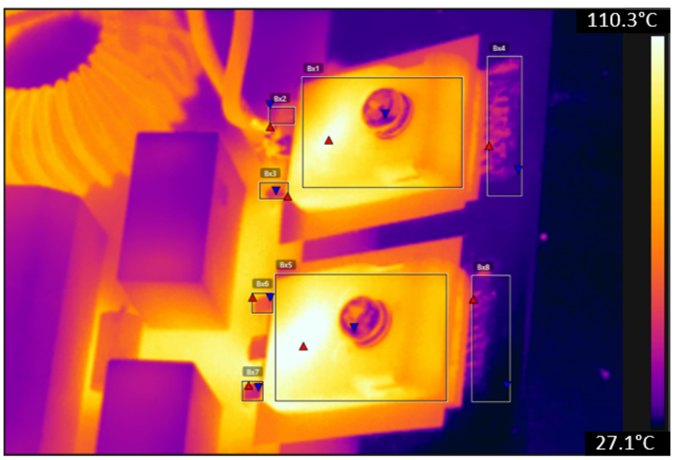

Fig. 3: IR camera image.

heating applications in the home appliance sector. The converter consists of a diode rectifier and two single-phase half-bridge inverters connected to different coils. To verify accuracy, the adopted measurement system utilized an infrared (IR) thermal camera on the open device, as depicted in Fig. 2. Specifically, the IR camera was used to observe temperature hotspots on the IGBT cases, output pins, and heatsink near the soldering points, providing a granular temperature map around the point of interest, i.e., the junction temperature which cannot be directly measured Fig. 3.

B. Applied Approach

For the specific application, a nominal conduction and switching loss model, which averages the behaviors of different datasheets of the components, has been designed as described in Section. II-A1. The outputs of the loss model constitute part of the inputs of the thermal model, specifically the heat sources. The thermal model comprises a 3D finite element thermal model that solves the heat equation neglecting the radiation component, making MOR techniques more effective.

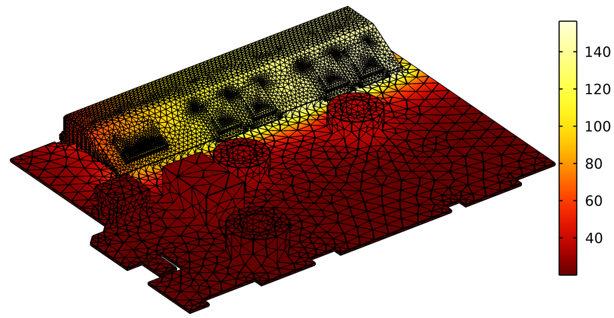

Fig. 4: Full Order Model. Temperature distribution in °C.

To reduce the finite element model, commercial software produced by Newtwen® has been adopted, implementing MOR techniques, as mentioned in the previous section, optimized for finite element matrices, which are typically large, sparse, and numerically ill-conditioned. The ROM is then implemented inside a low-power microprocessor as described in the following to validate its real-time feasibility.

The initial high-fidelity thermal model comprises approximately 10^5 Degrees of Freedom (DoF), see Fig. 4, while the final reduced order model (ROM) (obtained by using the Moment Matching technique [43], [48] with a convergence tolerance of 10^{-3} on the relative residual of the rhs of the problem) comprises only 20 DoF and is capable of describing the temperature at each node of the full order model (FOM) mesh with a maximum error of 2.5°C. The Moment Matching approach constructs the projection matrix by applying the Laplace transform to (5), i.e.,

$$\begin{aligned} s\mathbf{E}\mathbf{X}(s) &= \mathbf{A}\mathbf{X}(s) + \mathbf{B}\mathbf{U}(s) \\ \mathbf{Y}(s) &= \mathbf{C}\mathbf{X}(s) \end{aligned}, \tag{8}$$

where $s \in \mathbb{C}$ is the generalized frequency, and $\mathbf{X}$, $\mathbf{U}$, $\mathbf{Y}$ are the Laplace transform of $\mathbf{x}(t)$, $\mathbf{u}(t)$, and $\mathbf{y}(t)$, respectively. Then, the projection matrix $\mathbf{V}$ is constructed as

$$\mathbf{V} = [\mathbf{m}_0^1, \cdots, \mathbf{m}_p^k, \cdots, \mathbf{m}_P^N], \tag{9}$$

where $\mathbf{m}_p^k$ is the kp-th moment of (8) given as

$$\mathbf{m}_p^k = ((\mathbf{A} - s_k\mathbf{E})^{-1}\mathbf{E})^p(\mathbf{A} - s_k\mathbf{E})^{-1}\mathbf{B}, \tag{10}$$

where $p = 0, \cdots, P$ indicates the order, and $k = 1, \cdots, N$ the selected frequency (expansion point). However, a single thermal model is not sufficient to define a DT capable of accurately estimating the behavior of the real device, which can incorporate different components and operate under various load and boundary conditions, including varying cooling and environmental conditions over time. To address this issue, the physical model has been augmented with a data-driven model consisting of two FFNNs with distinct functions. As depicted in Fig. 1, the first neural network takes as input the input of the loss model and the thermal dynamics of temperature estimated by the thermal model at over 10 nodes of the mesh, as well as the real-time temperature measured by two NTC sensors implemented in the system. Its output is the correction of the input vector for the thermal model (i.e., the power

This article has been accepted for publication in IEEE Transactions on Power Electronics. This is the author's version which has not been fully edited and content may change prior to final publication. Citation information: DOI 10.1109/TPEL.2025.3531695

TABLE I: Experiments description

Experiment Set [cal/val/test]	Power min/max [W]	Current-Frequency [A/kHz]	Power profile [step/multi-level]	Supplier [1/2/3]	Figure -	Note -
cal.1	4200	80 / 18	step	1	Fig. 5	-
cal.2	3600	72 / 21	step	1	Fig. 6	-
cal.3	3600	75 / 22	step	1	Fig. 7	-
cal.4	4200	80 / 18	step	2	Fig. 8	-
cal.5	4200	80 / 18	step	3	Fig. 9	-
cal.6	3600	72 / 21	step	3	Fig. 10	-
val.1	4200	80 / 18	step	1	Fig. 11	-
val.2	3600	75 / 22	step	2	Fig. 12	-
test.1	480/3200	*	multi-level	1	Fig. 13	On/Off and different sequential power levels
test.2	480/3200	*	multi-level	2	Fig. 14	On/Off profile at different power levels
test.3	480/3200	*	multi-level	3	Fig. 15	Sequential power level and automatic control fan

losses), aiming to mitigate the errors of the loss model and uncertainties of boundary conditions, such as cooling fan speed and external temperature for convective heat exchange. In addition, the second neural network (with the same input as the first FFNN) serves to correct the final estimates of the thermal model-FFNN1 architecture, mitigating model errors stemming from material parameter uncertainties such as thermal capacity and conductivity, as well as variance due to multiple suppliers of power modules. Therefore, FFNN2 acts as the data-driven discrepancy model that enhances the generalization of the DT, maximizing its capability to represent the system under study and analysis. This hybrid model architecture allows for training the neural networks on a reduced dataset and, importantly, designing them with a limited number of layers and neurons, making them suitable for real-time implementation on microcontrollers.

C. *Model Accuracy*

Several experiments with very different working conditions have been done. Table I summarizes the relevant information of all the experiments reported in this section. In particular, 8 experiments have been used for the optimization of the two FFNNs, 6 of them for calibration (calibration set) and the remaining two for the validation and the best model selection (validation set). Three experiments have been used to finally test the hybrid DT in different and unseen working conditions.

To show the necessity of the inclusion of the FFNNs in the model, in Fig. 5–Fig. 15, the temperature estimation of the physics-based model (loss model + thermal ROM) only are included. Results show that introducing the data-driven part (i.e., the FFNNs) is mandatory to reach good accuracy, addressing the stochastic nature of the electric component.

The calibration dataset was generated from six different tests at various current levels and load conditions for each type of discrete component supplier. In Figs. 5 - 10, one can observe the results of the calibration. The loss function used is the Euclidean norm of the error between measurement and estimation at each moment of acquisition during the heating transient at three different geometric points corresponding to the temperature hot spots on the IGBT cases and the positioning of NTC sensors in the system. This allows for appropriately modeling the thermal gradient in the area of interest to make the estimation of junction temperature as reliable as possible, which is engineering-wise impossible to measure in the case of discrete components.

Maintaining a certain degree of generalization in the model architecture is essential to prevent overfitting and increase reliability. Overfitting occurs when the model learns to mem-

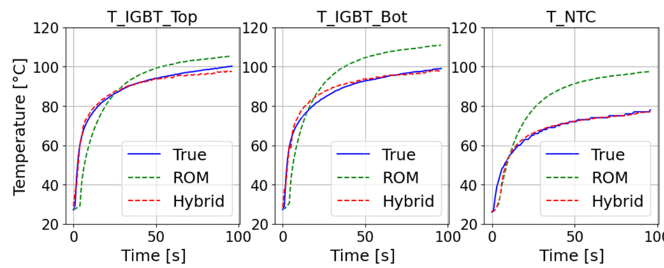

Fig. 5: Calibration Set: IGBT supplier 1, current-frequncy operational load 80 A / 18 kHz.

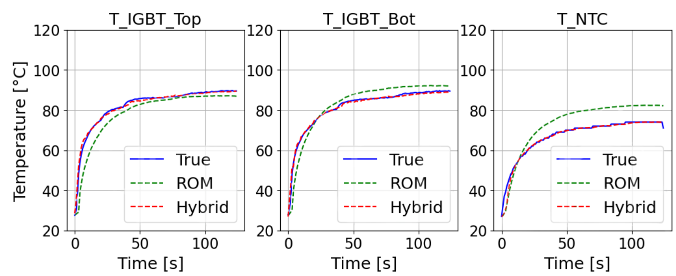

Fig. 6: Calibration Set: IGBT supplier 1, current-frequency operational load 72 A / 21 kHz.

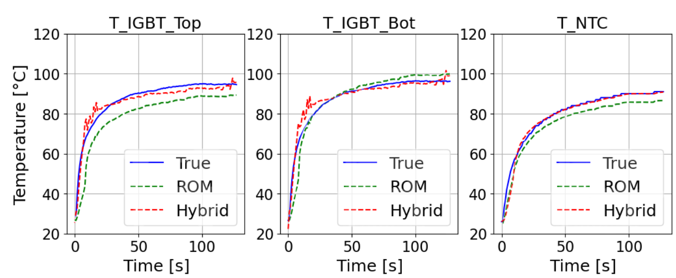

Fig. 7: Calibration Set: IGBT supplier 1, current-frequency operational load 75 A / 22 kHz.

This article has been accepted for publication in IEEE Transactions on Power Electronics. This is the author's version which has not been fully edited and content may change prior to final publication. Citation information: DOI 10.1109/TPEL.2025.3531695

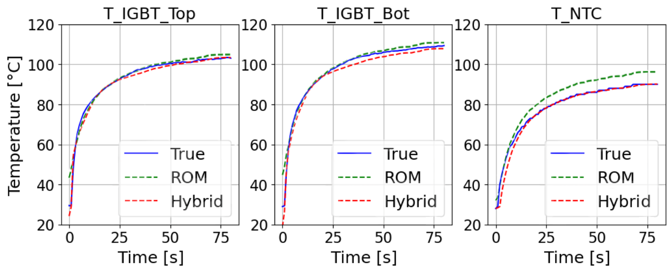

Fig. 8: Calibration Set: IGBT supplier 2, current-frequency operational load 80 A / 18 kHz.

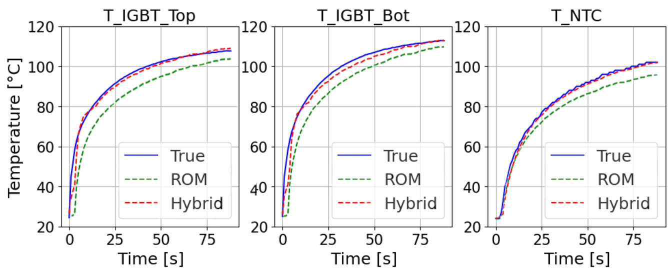

Fig. 9: Calibration Set: IGBT supplier 3, current-frequency operational load 80 A / 18 kHz.

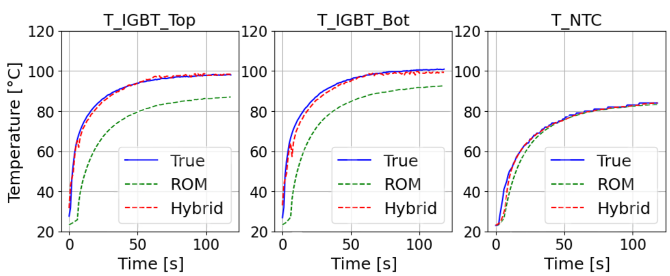

Fig. 10: Calibration Set: IGBT supplier 3, current-frequency operational load 72 A / 21 kHz.

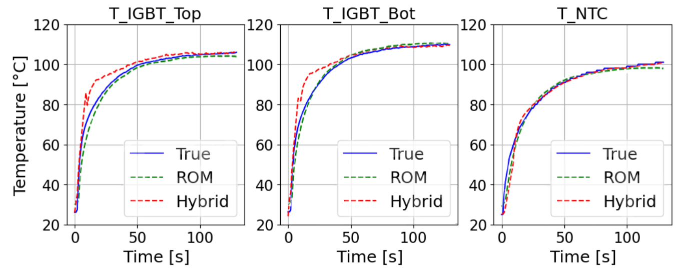

Fig. 11: Validation Set: IGBT supplier 1, current-frequency operational load 80 A / 18 kHz.

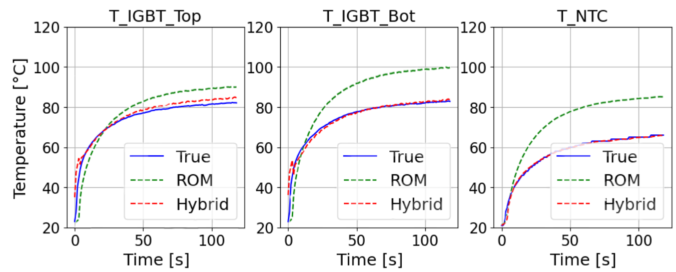

Fig. 12: Validation Set: IGBT supplier 3, current-frequency operational load 75 A / 22 kHz.

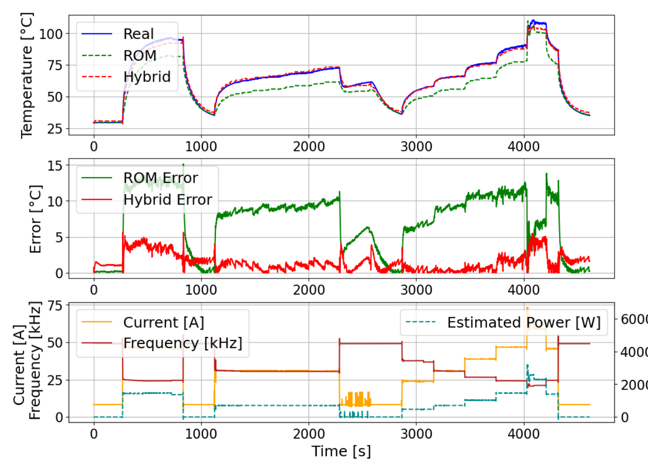

Fig. 13: Test Set: IGBT supplier 1, sequential multi-level profile.

orize training data rather than capturing underlying patterns, leading to poor generalization. By incorporating physics-based constraints, the model is less likely to extrapolate erroneously and more capable of making accurate predictions in diverse operating scenarios. To evaluate the generalization capability of the final model architecture, it is crucial to validate its performance in operating scenarios never seen during the calibration phase. This ensures that the model can effectively extrapolate beyond the training data and provides confidence in its reliability for real-world applications. For this purpose, in Fig. 11 and Fig. 12 one can observe the two validation sets at different operating conditions that have been used to check the generality of the approach.

Figs. 5-12 show the high accuracy of the developed physics-based data-driven augmented DT w.r.t. the measurements collected from three power converters, each one equipped with one of the three discrete components. Moreover, it is worth noting that, because using three different IGBTs, the temperature measured in the three power converters is very different, discrepancies of about 20°C can be spotted by comparing results of, e.g., Fig. 5, Fig. 8, and Fig. 9. However, for all of these conditions, the physics-based data-driven augmented DT is in perfect agreement with measurements.

After the optimization phase several experiments have been performed, to test the hybrid's capability model in different and unseen working performed. Among these experiments, the results of three representative cases are reported in Figs. 13, 14, and 15, where, for clarity of presentation, only the IGBT Top temperature measurements are shown, referring to the component case temperature as these were directly observable through the IR thermal camera measurements described in Section III.

In particular, these experiments are performed by applying complex working conditions, e.g., sequence of steps with different power levels, on-off power profile with different

This article has been accepted for publication in IEEE Transactions on Power Electronics. This is the author's version which has not been fully edited and content may change prior to final publication. Citation information: DOI 10.1109/TPEL.2025.3531695

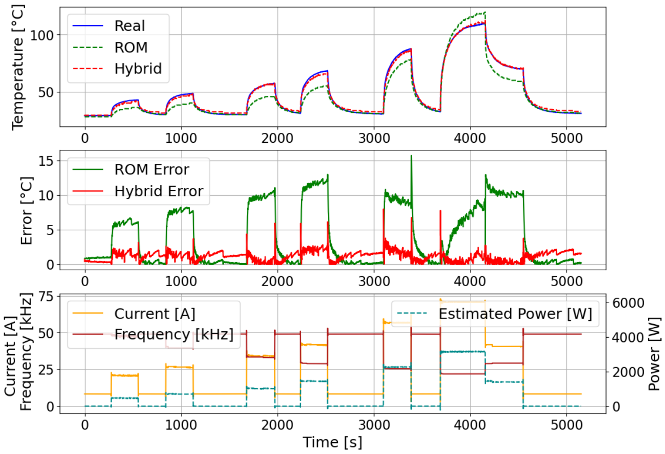

Fig. 14: Test Set: IGBT supplier 1, on/off profile.

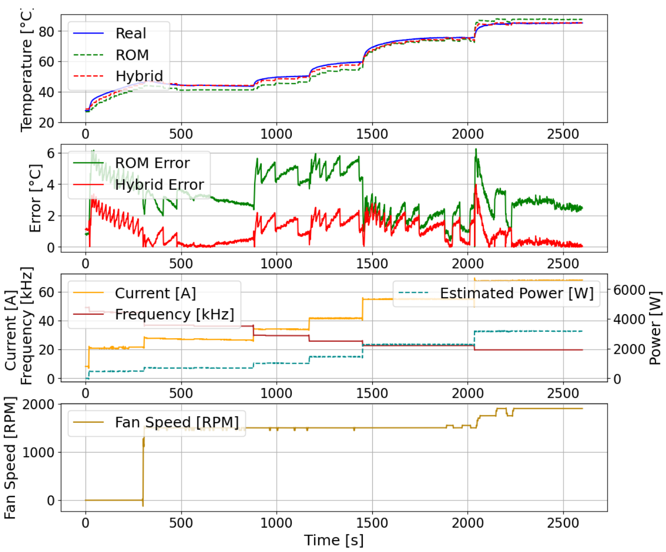

Fig. 15: Test Set: IGBT supplier 1, sequential multi-level profile with automatic fan control.

power levels, and the activation of the automatic fan controller. This allows us to test the performance of the hybrid DT with industrially relevant power profiles and different boundary conditions w.r.t. the ones accounted for during the optimization phase. The results show a very high accuracy of the hybrid DT, demonstrating that the proposed physic- and AI-based model structure can be trained even with experiments coming solely from simple scenarios without compromising its accuracy in monitoring industrially relevant conditions.

D. Computational Effort

The offline computational cost of this approach includes the effort required to construct the FEM model, perform its subsequent reduction through Moment Matching, and train the FFNNs. Computation were performed on a CPU Intel Core i7-1355u, 1.7GHz. The FEM model has a size of 10^5 DoF and the application of the Moment Matching reduction techniques leads to a 20 DoF reduced order model (convergence tolerance of 10^{-3}). The computation time to construct the FEM and generate the ROM was about 20 min. Thus, the reduced state space model is described by the following matrices: $\mathbf{A} = [20 \times 20]$, $\mathbf{B} = [20 \times 5]$, $\mathbf{C} = [10 \times 20]$. As is often the case, the human effort and time required to set up the FEM model far exceed the actual computational time needed to generate the ROM, with the human effort being particularly difficult to quantify. Alternatively, a data-driven approach (e.g., Vector Fitting or training Foster or Cauer networks) can drastically reduce the setup time, provided there is a solid understanding of the component's thermal behavior.

The total of the FFNNs parameters is 237 adopting Leaky Rectified Linear Unit (ReLU) activation functions, suitable for embedded implementation. The computation time needed for the overall train and validation of the FFNNs was approximatively 45 min.

Concerning the online computation time, the final hybrid model architecture is executed on an STM32-based evaluation board with an execution time of about 100 µs (65% of the overall time is required for the computation of the ROM, and the remaining 35% for the data-driven part, i.e., FFNNs) and 5 kB memory footprint in total. The microcontroller task implementing the DT operates with a cycle time of 10 ms, which is sufficiently fast to track the thermal dynamics of the component. The DT consumes only 1% of the microcontroller's computation time of the task where the DT is implemented (100 us vs 10 ms of the task), making it fully compatible with real-time execution requirements.

E. Discussion and Added Value

The real-time feasibility, accuracy, and level of generalization achieved allow for the implementation of a virtual temperature sensors system in production, which can be utilized for enhancing power derating performance by finely modulating switching frequency and current to maximize the product's state of function, i.e., increasing the functional burden of components by reducing safety margins through continuous monitoring of junction temperature. Moreover, although aging and degradation phenomena are outside the scope of this paper, it is worth mentioning that exploiting the increased quantity and quality of relevant information unlocked by the proposed hybrid DT (e.g., estimates in inaccessible points, spatial temperature gradients, cross-play of data between virtual and real sensors) provide useful information to develop aging and degradation models and identify reliable patterns with reduced costs and time. The temperature data obtained from NTC sensors (i.e., T_{NTC}) combined with DT predictions can be leveraged to predict component failures, aging, and degradation. However, addressing these phenomena requires the use of empirical formulas and assumptions that must be rigorously validated through experimental tests and dedicated studies. These experiments are essential to establish correlations between real and virtual sensor data with the actual occurrence of failures, aging, and degradation. Finally, various techniques should be explored to accurately and robustly identify these phenomena. For instance, recent literature has proposed the use of a particle swarm optimization algorithm coupled with a dual extended Kalman filter for online monitoring of the state of health of power semiconductors [5]. However, with the rise of AI-based methods, it is anticipated that new approaches will continue to emerge.

IV. Conclusions

In this paper, a comprehensive approach to constructing highly accurate and computationally efficient Digital Twins (DTs) of power electronics applications for the real-time monitoring of critical temperature has been proposed. Physics-based models are the starting point of the proposed work-flow, that are then reduced by using Model Order Reduction techniques to make the DT compatible with real-time execution on microprocessors. Finally, the real-time DT model is augmented by using Data-Driven Artificial Intelligence (AI)-based technique to improve its predictive reliability.

The effectiveness of the approach is verified using real-world power electronic converters intended for induction heating home appliance applications. These converters incorporate IGBTs sourced from various suppliers. Due to industry-wide supply shortages, it is common for manufacturers to utilize components from different suppliers, resulting in potential variability between otherwise equivalent products. Consequently, model-based monitoring becomes more complex. Nevertheless, the physics-based AI-augmented DT developed through the proposed approach exhibits excellent predictive reliability even in such realistic scenarios. This underscores the maturity and practical applicability of the proposed methodology in addressing challenges encountered in industrial settings.

References

[1] H. Chen, Z. Zhang, P. Karamanakos, and J. Rodriguez, "Digital twin techniques for power electronics-based energy conversion systems: A survey of concepts, application scenarios, future challenges, and trends," *IEEE Industrial Electronics Magazine*, vol. 17, no. 2, pp. 20–36, 2023.

[2] P. Karamanakos, E. Liegmann, T. Geyer, and R. Kennel, "Model predictive control of power electronic systems: Methods, results, and challenges," *IEEE Open Journal of Industry Applications*, vol. 1, pp. 95–114, 2020.

[3] S. Zhao and H. Wang, "Enabling data-driven condition monitoring of power electronic systems with artificial intelligence: Concepts, tools, and developments," *IEEE Power Electronics Magazine*, vol. 8, no. 1, pp. 18–27, 2021.

[4] B. Rodriguez, E. Sanjurjo, M. Tranchero, C. Romano, and F. Gonzalez, "Thermal parameter and state estimation for digital twins of e-powertrain components," *IEEE Access*, vol. 9, pp. 97 384–97 400, 2021.

[5] J. Kuprat, K. Debbadi, J. Schaumburg, M. Liserre, and M. Langwasser, "Thermal digital twin of power electronics modules for online thermal parameter identification," *IEEE Journal of Emerging and Selected Topics in Power Electronics*, vol. 12, no. 1, pp. 1020–1029, 2024.

[6] J. Kuprat, C. H. van der Broeck, M. Andresen, S. Kalker, M. Liserre, and R. W. De Doncker, "Research on active thermal control: Actual status and future trends," *IEEE Journal of Emerging and Selected Topics in Power Electronics*, vol. 9, no. 6, pp. 6494–6506, 2021.

[7] N. Baker, M. Liserre, L. Dupont, and Y. Avenas, "Improved reliability of power modules: A review of online junction temperature measurement methods," *IEEE Industrial Electronics Magazine*, vol. 8, no. 3, pp. 17–27, 2014.

[8] M. Andresen, K. Ma, G. Buticchi, J. Falck, F. Blaabjerg, and M. Liserre, "Junction temperature control for more reliable power electronics," *IEEE Transactions on Power Electronics*, vol. 33, no. 1, pp. 765–776, 2018.

[9] C. H. van der Broeck, L. A. Ruppert, R. D. Lorenz, and R. W. De Doncker, "Methodology for active thermal cycle reduction of power electronic modules," *IEEE Transactions on Power Electronics*, vol. 34, no. 8, pp. 8213–8229, 2019.

[10] K. Ma, M. Liserre, F. Blaabjerg, and T. Kerekes, "Thermal loading and lifetime estimation for power device considering mission profiles in wind power converter," *IEEE Transactions on Power Electronics*, vol. 30, no. 2, pp. 590–602, 2015.

[11] M. Andresen, M. Liserre, and G. Buticchi, "Review of active thermal and lifetime control techniques for power electronic modules," in *2014 16th European Conference on Power Electronics and Applications*, 2014, pp. 1–10.

[12] C. H. van der Broeck, T. A. Polom, R. D. Lorenz, and R. W. De Doncker, "Real-time monitoring of thermal response and life-time varying parameters in power modules," *IEEE Transactions on Industry Applications*, vol. 56, no. 5, pp. 5279–5291, 2020.

[13] S. Lohrasbi, R. Hammer, W. Essl, G. Reiss, S. Defregger, and W. Sanz, "A comprehensive review on the core thermal management improvement concepts in power electronics," *IEEE Access*, vol. 8, pp. 166 880–166 906, 2020.

[14] S. Jones-Jackson, R. Rodriguez, Y. Yang, L. Lopera, and A. Emadi, "Overview of current thermal management of automotive power electronics for traction purposes and future directions," *IEEE Transactions on Transportation Electrification*, vol. 8, no. 2, pp. 2412–2428, 2022.

[15] M. Andresen and M. Liserre, "Impact of active thermal management on power electronics design," *Microelectronics Reliability*, vol. 54, no. 9, pp. 1935–1939, 2014, sI: ESREF 2014.

[16] Y. Zhou, W. Shi, J. Tang, X. Wang, W. Li, X. He, C. Zhang, and Z. Li, "Dynamic junction temperature estimation via built-in negative thermal coefficient (ntc) thermistor in high power igbt modules," in *2017 IEEE Applied Power Electronics Conference and Exposition (APEC)*, 2017, pp. 772–775.

[17] S. Pyo and K. Sheng, "Junction temperature dynamics of power mosfet and sic diode," in *2009 IEEE 6th International Power Electronics and Motion Control Conference*, 2009, pp. 269–273.

[18] H. Chen, B. Ji, V. Pickert, and W. Cao, "Real-time temperature estimation for power mosfets considering thermal aging effects," *IEEE Transactions on Device and Materials Reliability*, vol. 14, no. 1, pp. 220–228, 2014.

[19] I. F. Kovačević, U. Drofenik, and J. W. Kolar, "New physical model for lifetime estimation of power modules," in *The 2010 International Power Electronics Conference - ECCE ASIA -*, 2010, pp. 2106–2114.

[20] S. Kalker, L. A. Ruppert, C. H. van der Broeck, J. Kuprat, M. Andresen, T. A. Polom, M. Liserre, and R. W. De Doncker, "Reviewing thermal-monitoring techniques for smart power modules," *IEEE Journal of Emerging and Selected Topics in Power Electronics*, vol. 10, no. 2, pp. 1326–1341, 2022.

[21] F. Stella, G. Pellegrino, E. Armando, and D. Daprà, "Online junction temperature estimation of sic power mosfets through on-state voltage mapping," *IEEE Transactions on Industry Applications*, vol. 54, no. 4, pp. 3453–3462, 2018.

[22] M. H. M. Sathik, J. Pou, S. Prasanth, V. Muthu, R. Simanjorang, and A. K. Gupta, "Comparison of igbt junction temperature measurement and estimation methods-a review," in *2017 Asian Conference on Energy, Power and Transportation Electrification (ACEPT)*, 2017, pp. 1–8.

[23] C. H. van der Broeck, A. Gospodinov, and R. W. De Doncker, "Igbt junction temperature estimation via gate voltage plateau sensing," *IEEE Transactions on Industry Applications*, vol. 54, no. 5, pp. 4752–4763, 2018.

[24] H. Wang, R. Zhu, H. Wang, M. Liserre, and F. Blaabjerg, "A thermal modeling method considering ambient temperature dynamics," *IEEE Transactions on Power Electronics*, vol. 35, no. 1, pp. 6–9, 2020.

[25] S. Kalker, C. H. van der Broeck, and R. W. De Doncker, "Online junction-temperature sensing of sic mosfets with minimal calibration effort," in *PCIM Europe digital days 2020; International Exhibition and Conference for Power Electronics, Intelligent Motion, Renewable Energy and Energy Management*, 2020, pp. 1–7.

[26] D. Hartmann, M. Herz, and U. Wever, "Model order reduction a key technology for digital twins," *Reduced-Order Modeling (ROM) for Simulation and Optimization: Powerful Algorithms as Key Enablers for Scientific Computing*, pp. 167–179, 2018.

[27] F. Di Napoli, A. Magnani, M. Coppola, P. Guerriero, V. D'Alessandro, L. Codecasa, P. Tricoli, and S. Daliento, "On-line junction temperature monitoring of switching devices with dynamic compact thermal models extracted with model order reduction," *Energies*, vol. 10, no. 2, 2017.

[28] M. G. Kapteyn, D. J. Knezevic, and K. Willcox, *Toward predictive digital twins via component-based reduced-order models and interpretable machine learning*. AIAA Scitech 2020 Forum, 2020.

[29] D. Hartmann, M. Herz, and U. Wever, *Model Order Reduction a Key Technology for Digital Twins*. Cham: Springer International Publishing, 2018, pp. 167–179.

[30] S. L. Brunton and J. N. Kutz, *Data-Driven Science and Engineering: Machine Learning, Dynamical Systems, and Control*. Cambridge University Press, 2019.

[31] M. Tezzele, N. Demo, A. Mola, and G. Rozza, *An integrated data-driven computational pipeline with model order reduction for industrial and applied mathematics*. Cham: Springer International Publishing, 2022, pp. 179–200.

[32] U. Drofenik and J. Kolar, "A general scheme for calculating switching- and conduction-losses of power semiconductors in numerical circuit simulations of power electronic systems," *Power Electronic Systems Laboratory (PES), ETH Zurich ETH-Zentrum, Zurich*, 2005.

[33] M. Zorzetto, R. Torchio, F. Lucchini, S. Maseei, L. Robol, and F. Dughiero, "Reduced order modeling for thermal simulations of electric components with surface-to-surface radiation," *IEEE Access*, 2024.

[34] L. Codecasa, "A novel approach for generating boundary condition independent compact dynamic thermal networks of packages," *IEEE Transactions on Components and Packaging Technologies*, vol. 28, no. 4, pp. 593–604, 2005.

[35] R. Codina, "On stabilized finite element methods for linear systems of convection diffusion reaction equations," *Computer Methods in Applied Mechanics and Engineering*, vol. 188, no. 1, pp. 61–82, 2000.

[36] A. P. Catalano, C. Scognamillo, V. d'Alessandro, and A. Castellazzi, "Numerical simulation and analytical modeling of the thermal behavior of single- and double-sided cooled power modules," *IEEE Transactions on Components, Packaging and Manufacturing Technology*, vol. 10, no. 9, pp. 1446–1453, 2020.

[37] B. Gustavsen and A. Semlyen, "Rational approximation of frequency domain responses by vector fitting," *IEEE Transactions on Power Delivery*, vol. 14, no. 3, pp. 1052–1061, 1999.

[38] T. Schütze, "AN2008-03: Thermal Equivalent Circuit Models," Infineon Technologies AG, Germany, Application Note, 2008.

[39] D. C. Wilcox, "Formulation of the k-w turbulence model revisited," *AIAA Journal*, vol. 46, no. 11, pp. 2823–2838, 2008.

[40] C. H. van der Broeck, M. Conrad, and R. W. De Doncker, "A thermal modeling methodology for power semiconductor modules," *Microelectronics Reliability*, vol. 55, no. 9, pp. 1938–1944, 2015, proceedings of the 26th European Symposium on Reliability of Electron Devices, Failure Physics and Analysis.

[41] C. H. van der Broeck, L. A. Ruppert, A. Hinz, M. Conrad, and R. W. De Doncker, "Spatial electro-thermal modeling and simulation of power electronic modules," *IEEE Transactions on Industry Applications*, vol. 54, no. 1, pp. 404–415, 2018.

[42] C. H. van der Broeck, R. D. Lorenz, and R. W. De Doncker, "Monitoring 3-d temperature distributions and device losses in power electronic modules," *IEEE Transactions on Power Electronics*, vol. 34, no. 8, pp. 7983–7995, 2019.

[43] L. Codecasa, D. D'Amore, and P. Maffezzoni, "Multipoint moment matching reduction from port responses of dynamic thermal networks," *IEEE Transactions on Components and Packaging Technologies*, vol. 28, no. 4, pp. 605–614, 2005.

[44] P. Benner, S. Grivet-Talocia, A. Quarteroni, G. Rozza, W. Schilders, and L. M. Silveira, Eds., *Model Order Reduction: Volume 1: System-and Data-Driven Methods and Algorithms*. Berlin, Germany: De Gruyter, 2021.

[45] T. Lassila, A. Manzoni, A. Quarteroni, and G. Rozza, *Model Order Reduction in Fluid Dynamics: Challenges and Perspectives*. Cham: Springer International Publishing, 2014, pp. 235–273.

[46] A. Ivagnes, G. Stabile, A. Mola, G. Rozza, and T. Iliescu, *Data Enhanced Reduced Order Methods for Turbulent Flows*. Cham: Springer Nature Switzerland, 2024, pp. 171–198.

[47] M. G. Kapteyn, J. V. R. Pretorius, and K. E. Willcox, "A probabilistic graphical model foundation for enabling predictive digital twins at scale," *Nature Computational Science*, vol. 1, no. 5, pp. 337–347, May 2021.

[48] X. Peng, Q. Bai, X. Xia, Z. Huang, K. Saenko, and B. Wang, "Moment matching for multi-source domain adaptation," in *Proceedings of the IEEE/CVF international conference on computer vision*, 2019, pp. 1406–1415.